MOEM

Modern Electronic Materials 2022; 8(1): 15–22
DOI 10.3897/j.moem.8.1.85251

Research Article

Degradation of the electrical conductivity of charged domain walls in reduced lithium niobate crystals

Aleksandr M. Kislyuk[1], Tatiana S. Ilina[1], Ilya V. Kubasov[1], Dmitry A. Kiselev[1], Aleksandr A. Temirov[1], Andrei V. Turutin[1], Andrey S. Shportenko[1], Mikhail D. Malinkovich[1], Yuri N. Parkhomenko[1,2]

1 National University of Science and Technology MISiS, 4-1 Leninsky Ave., Moscow 119049, Russia

2 Federal State Research and Develpment Institute of Rare Metal Industry (Giredmet JSC), 2 Elektrodnaya Str., Moscow 111524, Russia

Corresponding author: Aleksandr M. Kislyuk (akislyuk94@gmail.com)

Received 3 March 2022 ♦ **Accepted** 31 March 2022 ♦ **Published** 12 April 2022

Citation: Kislyuk AM, Ilina TS, Kubasov IV, Kiselev DA, Temirov AA, Turutin AV, Shportenko AS, Malinkovich MD, Parkhomenko YuN (2022) Degradation of the electrical conductivity of charged domain walls in reduced lithium niobate crystals. *Modern Electronic Materials* 8(1): 15–22. https://doi.org/10.3897/j.moem.8.1.85251

Abstract

In this work, the effect of long-term room temperature exposure on the electrical conductivity of the charged domain wall (CDWs) in nonpolar *x*-cut congruent lithium niobate ($LiNbO_3$, LN) crystals has been studied. Bidomain ferroelectric structures containing head-to-head charged domain boundaries have been produced by diffusion annealing in air near the Curie temperature and by infrared annealing. The crystals have been reduction annealed in a nitrogen atmosphere for the formation of color centers and growth of the electrical conductivity. The current measured during the recording of the I-V curves of the specimens using scanning probe microscope after room temperature exposure for 91 days has been found to decrease. The effect of storage conditions on the electrical conductivity of the CDWs has been studied. Degradation of the electrical conductivity does not originate from the effect of environment on the crystal surface. It has been hypothesized that the degradation is caused by distribution of charge carriers shielding the bound charge of the CDWs.

Keywords

lithium niobate, bidomain crystal, charged domain wall, diffusion annealing, piezoresponse force microscopy, reduction annealing.

1. Introduction

Domain walls are topographic defects in ferroics which separate domains having different random polarization directions. Lithium niobate ($LiNbO_3$, LN) show good promise for the fabrication of devices in which the unique properties of domain walls are implemented, because lithium niobate is a single-axis ferroelectric with 180-deg domain walls, high Curie temperature, refractory properties and chemical stability. The absence of lead in its composition and the availability of various diameter wafers and crystal cuts with reproducible properties in markets make this material one of the most industrially important ferroelectrics. Depending on the mutual orientation of random polarization vectors $\mathbf{P}_s$ adjacent domains may have three types of domain walls in LN: “head-to-tail”, “head-to-head” (H-H) and “tail-to-tail”. The charge of the domain wall is characterized by the angle θ between the direction of the vector $\mathbf{P}_s$ and the wall line, $0 < \theta < 90°$. The charge density at the

domain boundary is proportional to sin(θ) and hence charged domain walls **(CDWs)** with $|\theta| \approx 90°$ are the most charged ones [1–3]. The electrophysical properties of ferroelectric materials in the vicinity of CDW differ from those in the bulk thus raising both fundamental and applied interest to these objects. Although ferroelectric materials are wide-gap dielectrics, CDWs in these materials may have elevated electrical conductivity. The CDW are characterized by the presence of strong local electric fields induced by bound ion charge. Free carriers trapped by this electric field concentrate in the vicinity of the CDW hence potentially forming a conductive channel inside the dielectric material [4–6] or locally change the contact properties of the material [7]. The behavior of free carriers in the vicinity of CDW in some materials can be described by the model of quasi-2D electron gas, with the electrical conductivity being metallic [8, 9]. Atomic force microscopy methods allow local study of the electrophysical properties of the CDWs and the morphology of domains induced by applied bias to atomic force microscope **(AFM)** probe [10–12]. The possibility of forming high-density CDWs in ferroelectrics allows designing various electronic devices including new types of computer memory [13–15] and memristors which are promising for neuromorphic calculations [16–20]. For the fabrication of commercial devices on the basis of CDWs one should ensure reproducible and non-degradable electrophysical properties of domain boundaries in commercial products.

Multiple techniques of producing CDWs in LN single crystals have been reported. Most of them are based on the application of an external electric field which provides for local switching of the domain structure. Thus tilted partially charged domain walls form at an angle of $0 < \theta < 90°$ with the polar axis. Unfortunately the application of an external electric field from electrodes does not allow producing large-area CDWs with tilt angles of $\theta > 30°$ due to the growth of needle-shaped domains with jagged domain walls [1, 11, 21, 22]. Furthermore the dimensions and morphology of the domains forming in LN crystals under external electric field depend on polarization conditions and vary between different crystallographic cuts [23–25].

Another approach to the formation of CDWs in LN single crystals is to use force field gradients in the bulk. Examples of these fields are point defect or impurity atom concentrations as well as spatial temperature distribution upon cooling through the Curie point [26]. In this case the crystal wafer is split in two macrodomains separated by one CDW with $\theta \approx 90°$ (the so-called bidomain crystal). The domain inversion phenomenon in LN upon heat treatment in the vicinity of the Curie temperature accompanied by Li_2O out-diffusion was discovered [27, 28] and studied [29–34]. Along with diffusion annealing of LN crystals near the Curie point, bidomain ferroelectric structures can be alternatively produced by annealing of crystals subjected to proton exchange [35–38] and heat treatment of crystals in an inhomogeneous thermal field [39–42]. Bidomain crystals are also promising as materials for the fabrication of precision actuators [39, 43–49], low-frequency vibration gages [50] and magnetic field sensors (as a constituent of composite magnetoelectric materials) [51] as well as for waste heat power systems [52, 53].

LN is a good insulator and therefore most studies of CDWs use Mg doped crystals since Mg increases the electrical conductivity [3, 21, 54–56]. Currents in CDWs formed in Mg : LN can be further increased by super-bandgap photoexcitation [3, 56] and domain engineering [54]. Along with doping, an alternative approach to increasing the electrical conductivity of the crystals is annealing in a reducing environment (vacuum, hydrogen, nitrogen or inert atmosphere) [57–62]. Chemically reduced crystals become almost transparent, with a wide optical absorption band having a maximum at 2.5 eV which is attributed in literature to bound bipolarons [58, 63]. It has been found recently [7] that local switching of "head-to-head" CDW domain structures in LN crystals after reduction annealing provides for efficient control of AFM probe / CDW point contact conductivity. However the stability of the electrophysical properties of these domains has not been studied in detail yet. The aim of this work is to study the stability of the electrophysical properties of CDWs in reduced LN crystals.

2. Experimental

The test specimens were commercial congruent *z*-cut LN crystals (The Roditi International Corporation Ltd). The wafers were cut into rectangular $10 \times 10 \times 1$ mm^3 pieces that were further diffusion annealed in air [28, 33, 47] for the formation of a H-H bidomain ferroelectric structure. As a result a long CDW was formed in the middle of the bulk of the whole wafer. For AFM studies following the method described earlier [10, 29, 39], thin transverse cuts of the crystals were made so the polar axis is in the specimen plane and the nonpolar axis is perpendicular to the specimen surface. Thereafter one of the planes so obtained was sequentially polished with ASM3/2 diamond powder and cerium oxide powder with the main fraction size of 0.8 μm. For increasing the electrical conductivity and surface recrystallization after mechanical treatment the specimens were reduction annealed at 1030 °C for 60 min in a ULVAC VHC-P610 infrared furnace in 6.0 Grade dried nitrogen atmosphere (purity grade 99.9999%). After reduction annealing a chromium electrode was magnetron-sputtered onto the surface opposite to the polished side. Chromium forms an Ohmic contact to lithium niobate [64, 65]. The crystals were attached by the chromium electrode side to a metallic substrate using Leitsilber 200 conducting silver paste. The schematic of specimen preparation is shown in Fig. 1.

Study of the CDWs by piezoresponse force microscopy, conductive atomic force microscopy (c-AFM) and I-V curve recording methods was carried out under an

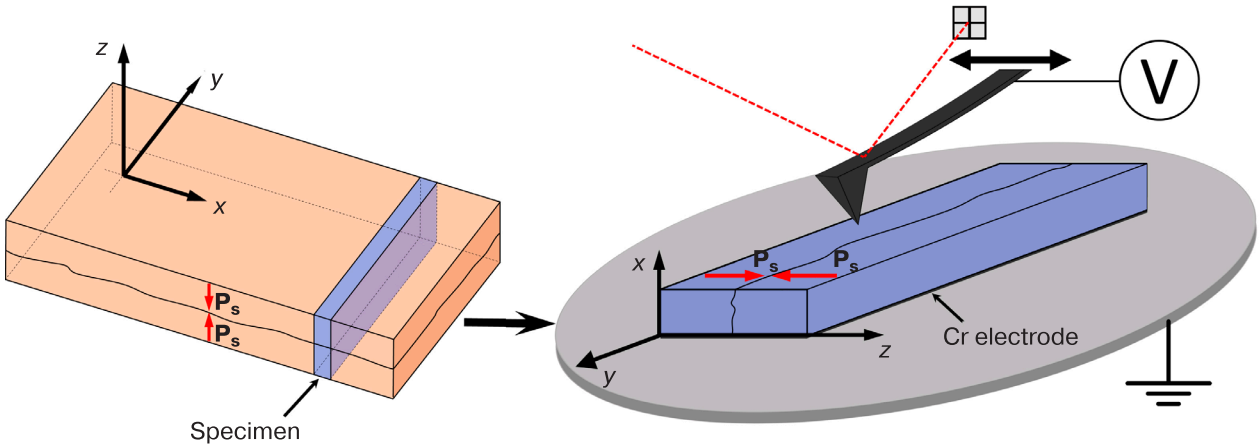

Figure 1. Schematic of specimen preparation.

Asylum Research MFP-3D Stand Alone probe microscope. High-resolution silicon cantilevers with NSG30/Pt platinum coating were used. The cantilever bias for c-AFM imaging of CDW areas was +7 V. For studying the time stability of the electrophysical properties of the CDWs in the LN bidomain crystals the I-V curves were recorded at several CDW points and c-AFM images were taken for the CDW crystal region immediately after reduction annealing and after long-term exposure for 91 days.

At the first phase of the study the threshold switching voltages of the domain structure were measured using the AFM probe. To this end, square pulses 20 sec ranging from 0 to ±200 V at a 10 V step were applied to different points of the monodomain region of the specimen. The domain structure was visualized using piezoresponse force microscopy. The results showed that the switching of the domain structure is caused by biasing of the cantilever with ≥+30 V and ≤–50 V. For avoiding repolarization during I-V curve measurement all the subsequent measurements were carried out in the –20 to +20 V range. The positive and negative I-V curve branches were taken separately at several CDW points. The I-V curves were taken from CDW regions with tilt angles close to 90 deg with a 10 sec sawtooth signal for 20 cycles, the data being averaged over the measurement cycles. Then the specimen was divided in two halves. For studying the effect of environment on the stability of the electrophysical properties of the CDWs one half of the specimen was placed into *n*-hexane and the other left in air. Hexane is a nonpolar aprotonic solvent that prevents the CDWs of the reduced crystal from oxidation in ambient oxygen and is supposed not to shield the CDWs field. The specimens were held in dark air-proof containers at room temperature. The temperature and humidity in the room were not stabilized. After exposure the I-V curves and c-AFM images were taken again.

3. Results and discussion

AFM topographic study of the bidomain LN crystal *x*-cut surface containing the H-H CDW showed that reduction annealing of the crystal smoothens the sur-

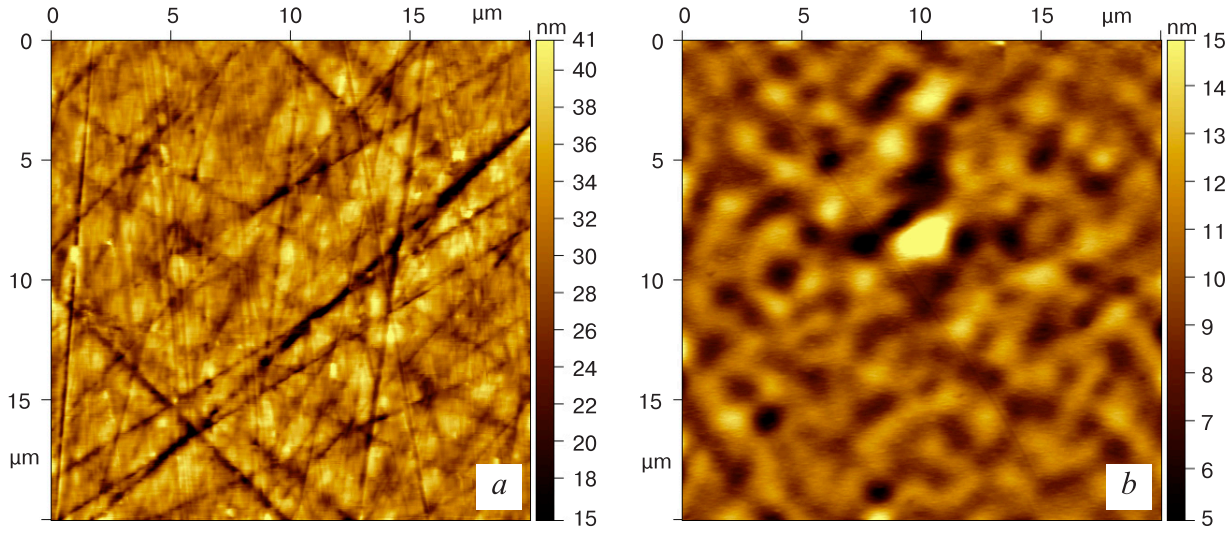

Figure 2. Topography of bidomain LN crystal *x*-cut (*a*) as-polished and (*b*) after reduction annealing.

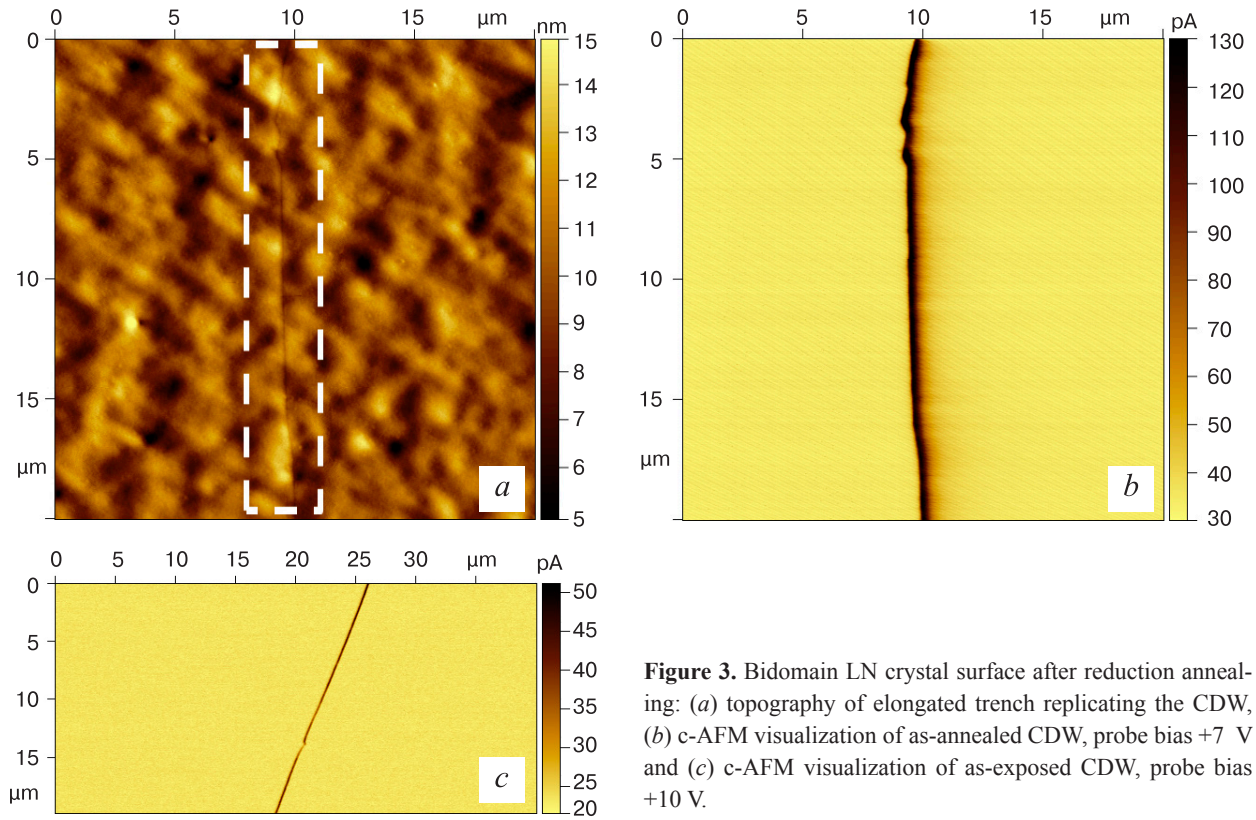

Figure 3. Bidomain LN crystal surface after reduction annealing: (*a*) topography of elongated trench replicating the CDW, (*b*) c-AFM visualization of as-annealed CDW, probe bias +7 V and (*c*) c-AFM visualization of as-exposed CDW, probe bias +10 V.

face and reduces the quantity of scratches (Fig. 2). The RMS surface roughness decreased from 5,59±1,56 nm to 2,91±1,06 nm. This change seemingly originates from specimen surface recrystallization.

The smoothening of the specimen surface roughness is accompanied by the formation of an elongated trench coincident with the CDW line in the c-AFM scan (Fig. 3 *a* and *b*). This phenomenon was described in literature earlier [66]. The depth of the trench was approximately 0.3 nm, its width being 70 nm. The formation of the elongated trench on the crystal surface can be caused by the more intense O_2 and Li_2O evaporation during annealing [67].

The c-AFM images taken with a +7 V probe bias before exposure allow visualizing the CDW (Fig. 3 *b*). However after exposure the current measured at the CDW at a +7 V bias was below the scanning probe microscope sensitivity. CDW visualization in the specimens after exposure in air and in *n*-hexane was achieved at a higher bias, i.e., +10 V (Fig. 3 *c*). The I-V curves taken after long exposure suggest degradation of the CDW electrical conductivity (Fig. 4). The current measured for the I-V curves of the CDW biased to +20 V decreased by almost one order of magnitude as a result of exposure. Noticeably there was no tangible difference in the I-V curves and the c-AFM images between the specimens exposed to air and to *n*-hexane.

After air and *n*-hexane exposure the surface of the specimens still had the trench and hence the degradation of the electrical conductivity was not caused by adhesion of contaminants. There were attempts to recover the electrical conductivity, but crystal surface cleaning with various solvents, fast etching in a mixture of hydrochloric and nitric acids and etching in ionized argon did not give any results. It should be noted that repeated surface polishing during reduction annealing restored the electrical conductivity to its initial high level.

In order to understand whether the degradation of the electrical conductivity has a surface or bulk origin the crystals were cleaved after exposure. Although the crystal's cleavage surface pattern differs considerably from

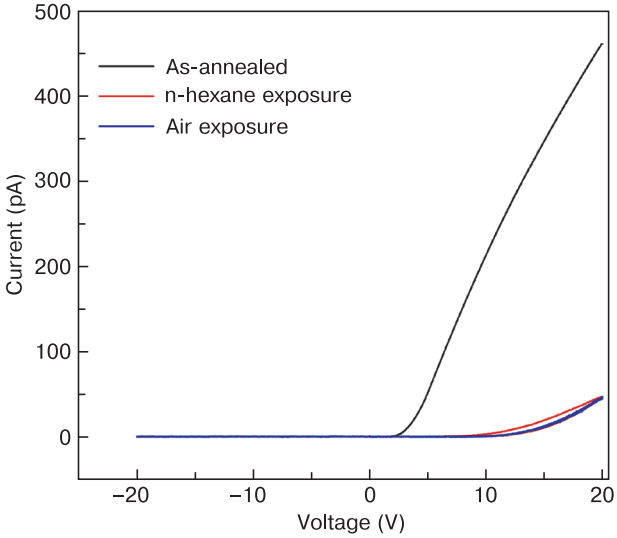

Figure 4. Comparison between I-V curves of reduced bidomain LN crystals as-reduced and after exposure in air and in *n*-hexane.

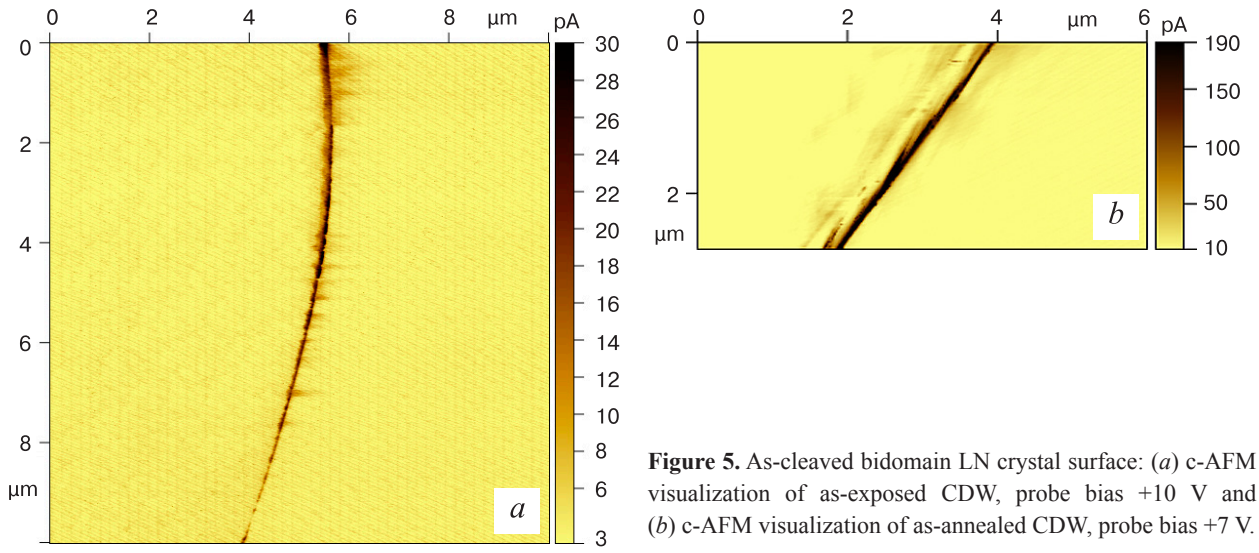

Figure 5. As-cleaved bidomain LN crystal surface: (*a*) c-AFM visualization of as-exposed CDW, probe bias +10 V and (*b*) c-AFM visualization of as-annealed CDW, probe bias +7 V.

the as-annealed surface pattern, the c-AFM scans for +10 V bias showed currents close to those for surface before cleaving (Fig. 5 *a*). However the crystals cleaved immediately after reduction annealing had a high CDW electrical conductivity (Fig. 5 *b*), i.e., electrical conductivity degradation occurs in the entire crystal bulk.

An experiment was set up in which electrical conductivity degradation was stimulated by radiation absorption near the crystal's self-absorption edge. The bidomain LN crystal after reduction annealing was irradiated with a solid-state 320 nm UV laser at a radiation power of 5 mW. UV radiation absorption by the crystal surface layers led to local heating and generation of hole polarons [68]. c-AFM study of the unirradiated and as-irradiated CDWs showed a dramatic degradation of the electrical conductivity down to the scanning probe microscope sensitivity threshold after 1 min irradiation. The c-AFM images of the as-irradiated LN crystal did not visualize the CDW for scans taken at a bias of below +20 V.

Chemical reduction of the lithium niobate crystals can be described with the following reaction formula [69]:

$$LiNbO_3 \leftrightarrow O_2 + Li_2O + Nb_{Li}^{4\bullet} + 4e^-.$$

Free conductivity band electrons are trapped by Nb_{Li} and Nb_{Nb} defects each of which forms a small-radius polaron. Eventually, Nb_{Li}^{4+} and Nb_{Nb}^{4+} polarons localized at adjacent lattice sites (along the polar axis) form a stable bound pair, i.e., a small-radius bipolaron $(Nb_{Li}^{4+}–Nb_{Nb}^{4+})^{2-}$ [59, 60, 69–71]. Presumably the conditions of bound bipolaron formation differ between the CDW and the single domain region.

4. Conclusion

The phenomenon of I-V curve current reduction was studied using AFM. The electrophysical properties of the bidomain LN crystals after reduction annealing proved to be unstable in time, the electrical conductivity decreasing by one order of magnitude after long-term exposure. This phenomenon was found to be not associated with the effect of environment on the surface; rather it is caused by redistribution of carriers shielding the bound charge of the CDW.

Acknowledgments

The reported study was funded by RFBR, project number 20-32-90141 on equipment of Materials Science and Metallurgy Joint Use Center in the NUST MISiS with financial support from the Ministry of Education and Science of the Russian Federation (No. 075-15-2021-696). The Authors acknowledges the Ministry of Education and Science of the Russian Federation for the support in the framework of the State Assignment (basic research, Project No. 0718-2020-0031).

References

1. Eliseev E.A., Morozovska A.N., Svechnikov G.S., Gopalan V., Shur V.Y. Static conductivity of charged domain walls in uniaxial ferroelectric semiconductors. *Physical Review B: Condensed Matter and Materials Physics*. 2011; 83(23): 235313. https://doi.org/10.1103/PhysRevB.83.235313
2. Wolba B., Seidel J., Cazorla C., Godau C., Haußmann A., Eng L.M. Resistor network modeling of conductive domain walls in lithium niobate. *Advanced Electronic Materials*. 2018; 4(1): 1700242. https://doi.org/10.1002/aelm.201700242
3. Schröder M., Haußmann A., Thiessen A., Soergel E., Woike T., Eng L.M. Conducting domain walls in lithium niobate single crys-

tals. *Advanced Functional Materials*. 2012; 22(18): 3936–3944. https://doi.org/10.1002/adfm.201201174

4. Werner C.S., Herr S.J., Buse K., Sturman B., Soergel E., Razzaghi C., Breunig I. Large and accessible conductivity of charged domain walls in lithium niobate. *Scientific Reports*. 2017; 7(1): 9862. https://doi.org/10.1038/s41598-017-09703-2
5. Vasudevan R.K., Wu W., Guest J.R., Baddorf A.P., Morozovska A.N., Eliseev E.A., Balke N., Nagarajan V., Maksymovych P., Kalinin S.V. Domain wall conduction and polarization-mediated transport in ferroelectrics. *Advanced Functional Materials*. 2013; 23(20): 2592—2616. https://doi.org/10.1002/adfm.201300085
6. Gureev M.Y., Tagantsev A.K., Setter N. Head-to-head and tail-to-tail 180° domain walls in an isolated ferroelectric. *Physical Review B: Condensed Matter and Materials Physics*. 2011; 83(18): 184104. https://doi.org/10.1103/PhysRevB.83.184104
7. Kubasov I.V., Kislyuk A.M., Ilina T.S., Shportenko A.S., Kiselev D.A., Turutin A.V., Temirov A.A., Malinkovich M.D., Parkhomenko Y.N. Conductivity and memristive behavior of completely charged domain walls in reduced bidomain lithium niobate. *Journal of Materials Chemistry C*. 2021; 9(43): 15591–15607. https://doi.org/10.1039/d1tc04170c
8. Sluka T., Tagantsev A.K., Bednyakov P., Setter N. Free-electron gas at charged domain walls in insulating $BaTiO_3$. *Nature Communications*. 2013; 4(1): 1808. https://doi.org/10.1038/ncomms2839
9. Vul B.M., Guro G.M., Ivanchik I.I. Encountering domains in ferroelectrics. *Ferroelectrics*. 1973; 6(1): 29–31. https://doi.org/10.1080/00150197308237691
10. Kislyuk A.M., Ilina T.S., Kubasov I.V., Kiselev D.A., Temirov A.A., Turutin A.A., Malinkovich M.D., Polisan A.A., Parkhomenko Yu.N. Formation of stable induced domains at charged domain boundary in lithium niobate using scanning probe microscopy. *Izvestiya Vysshikh Uchebnykh Zavedenii. Materialy Elektronnoi Tekhniki = Materials of Electronics Engineering*. 2019; 22(1): 5–17. (In Russ.). https://doi.org/10.17073/1609-3577-2019-1-5-17
11. Alikin D.O., Ievlev A.V., Turygin A.P., Lobov A.I., Kalinin S.V., Shur V.Y. Tip-induced domain growth on the non-polar cuts of lithium niobate single-crystals. *Applied Physics Letters*. 2015; 106(18): 182902. https://doi.org/10.1063/1.4919872
12. Schultheiß J., Rojac T., Meier D. Unveiling alternating current electronic properties at ferroelectric domain walls. *Advanced Electronic Materials*. 2022; 8(6): 2100996. https://doi.org/10.1002/aelm.202100996
13. Jiang A.-Q., Geng W.P., Lv P., Hong J., Jiang J., Wang C., Chai X.J., Lian J.W., Zhang Y., Huang R., Zhang D.W., Scott J.F., Hwang C.S. Ferroelectric domain wall memory with embedded selector realized in $LiNbO_3$ single crystals integrated on Si wafers. *Nature Materials*. 2020; 19(11): 1188–1194. https://doi.org/10.1038/s41563-020-0702-z
14. Wang C., Jiang J., Chai X., Lian J., Hu X., Jiang A.Q. Energy-efficient ferroelectric domain wall memory with controlled domain switching dynamics. *ACS Applied Materials & Interfaces*. 2020; 12(40): 44998–45004. https://doi.org/10.1021/acsami.0c13534
15. Qian Y., Zhang Z., Liu Y., Xu J., Zhang G. Graphical direct writing of macroscale domain structures with nanoscale spatial resolution in nonpolar-cut lithium niobate on insulators. *Journal of Applied Physics*. 2022; 17: 054049. https://doi.org/10.1103/PhysRevApplied.17.054049
16. Krestinskaya O., James A.P., Chua L.O. Neuromemristive circuits for edge computing: A review. *IEEE Transactions on Neural Networks and Learning Systems*. 2020; 31(1): 4–23. https://doi.org/10.1109/TNNLS.2019.2899262
17. Chaudhary P., Lu H., Lipatov A., Ahmadi Z., McConville J.P.V., Sokolov A., Shield J.E., Sinitskii A., Gregg J.M., Gruverman A. Low-voltage domain-wall $LiNbO_3$ memristors. *Nano Letters*. 2020; 20(8): 5873–5878. https://doi.org/10.1021/acs.nanolett.0c01836
18. McConville J.P.V., Lu H., Wang B., Tan Y., Cochard C., Conroy M., Moore K., Harvey A., Bangert U., Chen L., Gruverman A., Gregg J.M. Ferroelectric domain wall memristor. *Advanced Functional Materials*. 2020; 30(28): 2000109. https://doi.org/10.1002/adfm.202000109
19. Jiang J., Wang C., Chai X., Zhang Q., Hou X., Meng F., Gu L., Wang J., Jiang A.Q. Surface-bound domain penetration and large wall current. *Advanced Electronic Materials*. 2021; 7(3): 2000720. https://doi.org/10.1002/aelm.202000720
20. Maksymovych P., Seidel J., Chu Y.H., Wu P., Baddorf A.P., Chen L.-Q.Q., Kalinin S.V., Ramesh R. Dynamic conductivity of ferroelectric domain walls in $BiFeO_3$. *Nano Letters*. 2011; 11(5): 1906–1912. https://doi.org/10.1021/nl104363x
21. Lu H., Tan Y., McConville J.P.V., Ahmadi Z., Wang B., Conroy M., Moore K., Bangert U., Shield J.E., Chen L.Q., Gregg J.M., Gruverman A. Electrical tunability of domain wall conductivity in $LiNbO_3$ thin films. *Advanced Materials*. 2019; 31(48): 1902890. https://doi.org/10.1002/adma.201902890
22. Shur V.Y., Rumyantsev E.L., Nikolaeva E.V., Shishkin E.I. Formation and evolution of charged domain walls in congruent lithium niobate. *Applied Physics Letters*. 2000; 77(22): 3636–3638. https://doi.org/10.1063/1.1329327
23. Ievlev A.V., Alikin D.O., Morozovska A.N., Varenyk O.V., Eliseev E.A., Kholkin A.L., Shur V.Y., Kalinin S.V. Symmetry breaking and electrical frustration during tip-induced polarization switching in the nonpolar cut of lithium niobate single crystals. *ACS Nano*. 2015; 9(1): 769–777. https://doi.org/10.1021/nn506268g
24. Turygin A.P., Alikin D.O., Kosobokov M.S., Ievlev A.V., Shur V.Y. Self-organized formation of quasi-regular ferroelectric nanodomain structure on the nonpolar cuts by grounded SPM tip. *ACS Applied Materials & Interfaces*. 2018; 10(42): 36211–36217. https://doi.org/10.1021/acsami.8b10220
25. Ievlev A.V., Morozovska A.N., Shur V.Y., Kalinin S.V. Ferroelectric switching by the grounded scanning probe microscopy tip. *Physical Review B: Condensed Matter and Materials Physics*. 2015; 91(21): 214109. https://doi.org/10.1103/PhysRevB.91.214109
26. Kubasov I.V., Kislyuk A.M., Turutin A.V., Malinkovich M.D., Parkhomenko Y.N. Bidomain ferroelectric crystals: properties and prospects of application. *Russian Microelectronics*. 2021; 50(8): 571–616. https://doi.org/10.1134/S1063739721080035
27. Evlanova N.L., Rashkovich L.N. Annealing effect on domain-structure of lithium meta-niobate single-crystals. *Soviet Physics, Solid State*. 1974;16:354.
28. Ohnishi N. An etching study on a heat-induced layer at the positive-domain surface of $LiNbO_3$. *Japanese Journal of Applied Physics*. 1977; 16(6): 1069–1070. https://doi.org/10.1143/jjap.16.1069
29. Kubasov I.V., Timshina M.S., Kiselev D.A., Malinkovich M.D., Bykov A.S., Parkhomenko Y.N. Interdomain region in single-crystal lithium niobate bimorph actuators produced by light anneal-

ing. *Crystallography Reports*. 2015; 60(5): 700–705. https://doi.org/10.1134/S1063774515040136

30. Kubasov I.V., Kislyuk A.M., Bykov A.S., Malinkovich M.D., Zhukov R.N., Kiselev D.A., Ksenich S.V., Temirov A.A., Timushkin N.G., Parkhomenko Y.N. Bidomain structures formed in lithium niobate and lithium tantalate single crystals by light annealing. *Crystallography Reports*. 2016; 61(2): 258–262. https://doi.org/10.1134/S1063774516020115
31. Kugel V.D., Rosenman G. Domain inversion in heat-treated $LiNbO_3$ crystals. *Applied Physics Letters*. 1993; 62(23): 2902–2904. https://doi.org/10.1063/1.109191
32. Rosenman G., Kugel V.D., Shur D. Diffusion-induced domain inversion in ferroelectrics. *Ferroelectrics*. 1995; 172(1): 7–18. https://doi.org/10.1080/00150199508018452
33. Nakamura K., Ando H., Shimizu H. Partial domain inversion in $LiNbO_3$ plates and its applications to piezoelectric devices. In: *IEEE 1986 Ultrasonics Symposium*. Williamsburg, VA, USA. 17–19 November 1986. USA: IEEE; 2005: 719–722. https://doi.org/10.1109/ULTSYM.1986.198828
34. Nakamura K., Ando H., Shimizu H. Ferroelectric domain inversion caused in $LiNbO_3$ plates by heat treatment. *Applied Physics Letters*. 1987; 50(20): 1413–1414. https://doi.org/10.1063/1.97838
35. Nakamura K., Shimizu H. Ferroelectric inversion layers formed by heat treatment of proton-exchanged $LiTaO_3$. *Applied Physics Letters*. 1990; 56(16): 1535–1536. https://doi.org/10.1063/1.103213
36. Zhu Y.Y., Zhu S.N., Hong J.F., Ming N. Ben domain inversion in $LiNbO_3$ by proton exchange and quick heat treatment. *Applied Physics Letters*. 1994; 65(5): 558–560. https://doi.org/10.1063/1.112295
37. Zhang Z.Y., Zhu Y.Y., Zhu S.N., Ming N. Ben domain inversion by Li_2O out-diffusion or proton exchange followed by heat treatment in $LiTaO_3$ and $LiNbO_3$. *Physica Status Solidi A: Applied Research*. 1996; 153(1): 275–279. https://doi.org/10.1002/pssa.2211530128
38. Åhlfeldt H., Webjörn J., Arvidsson G. Periodic domain inversion and generation of blue light in lithium tantalate waveguides. *IEEE Photonics Technology Letters*. 1991; 3(7): 638–639. https://doi.org/10.1109/68.87938
39. Bykov A.S., Grigoryan S.G., Zhukov R.N., Kiselev D.A., Ksenich S.V., Kubasov I.V., Malinkovich M.D., Parkhomenko Y.N. Formation of bidomain structure in lithium niobate plates by the stationary external heating method. *Russian Microelectronics*. 2014; 43(8): 536–542. https://doi.org/10.1134/S1063739714080034
40. Tasson M., Legal H., Peuzin J.C., Lissalde F.C. Mécanismes d'orientation de la polarisation spontanée dans le niobate de lithium au voisinage du point de Curie. *Physica Status Solidi A: Applied Research*. 1975; 31(2): 729–737. https://doi.org/10.1002/pssa.2210310246
41. Tasson M., Legal H., Gay J.C., Peuzin J.C., Lissalde F.C. Piezoelectric study of poling mechanism in lithium niobate crystals at temperature close to the curie point. *Ferroelectrics*. 1976; 13(1): 479–481. https://doi.org/10.1080/00150197608236646
42. Luh Y.S., Feigelson R.S., Fejer M.M., Byer R.L. Ferroelectric domain structures in $LiNbO_3$ single-crystal fibers. *Journal of Crystal Growth*. 1986; 78(1): 135–143. https://doi.org/10.1016/0022-0248(86)90510-5
43. Blagov A.E., Bykov A.S., Kubasov I.V., Malinkovich M.D., Pisarevskii Y.V., Targonskii A.V., Eliovich I.A., Kovalchuk M.V. An electromechanical X-ray optical element based on a hysteresis-free monolithic bimorph crystal. *Instruments and Experimental Techniques*. 2016; 59(5): 728–732. https://doi.org/10.1134/S0020441216050043
44. Marchenkov N., Kulikov A., Targonsky A., Eliovich Y., Pisarevsky Y., Seregin A., Blagov A., Kovalchuk M. $LiNbO_3$-based bimorph piezoactuator for fast X-ray experiments: Resonant mode. *Sensors and Actuators A: Physical*. 2019; 293(10): 48–55. https://doi.org/10.1016/j.sna.2019.04.028
45. Kulikov A., Blagov A., Marchenkov N., Targonsky A., Eliovich Y., Pisarevsky Y., Kovalchuk M. $LiNbO_3$-based bimorph piezoactuator for fast X-ray experiments: Static and quasistatic modes. *Sensors and Actuators A: Physical*. 2019; 291(6): 68–74. https://doi.org/10.1016/j.sna.2019.03.041
46. Nakamura K., Ando H., Shimizu H. Bending Vibrator consisting of a $LiNbO_3$ plate with a ferroelectric inversion layer. *Japanese Journal of Applied Physics*. 1987; 26(S2): 198. https://doi.org/10.7567/JJAPS.26S2.198
47. Nakamura K., Shimizu H. Hysteresis-free piezoelectric actuators using $LiNbO_3$ plates with a ferroelectric inversion layer. *Ferroelectrics*. 1989; 93(1): 211–216. https://doi.org/10.1080/00150198908017348
48. Nakamura K. Antipolarity domains formed by heat treatment of ferroelectric crystals and their applications. *Japanese Journal of Applied Physics*. 1992; 31(S1): 9–13. https://doi.org/10.7567/JJAPS.31S1.9
49. Nakamura K., Nakamura T., Yamada K. Torsional actuators using $LiNbO_3$ plates with an inversion layer. *Japanese Journal of Applied Physics*. 1993; 32(5S): 2415–2417. https://doi.org/10.1143/JJAP.32.2415
50. Kubasov I.V., Kislyuk A.M., Turutin A.V., Bykov A.S., Kiselev D.A., Temirov A., Zhukov R.N., Sobolev N.A., Malinkovich M.D., Parkhomenko Y.N. Low-frequency vibration sensor with a sub-nm sensitivity using a bidomain lithium niobate crystal. *Sensors (Switzerland)*. 2019; 19(3): 614. https://doi.org/10.3390/s19030614
51. Turutin A.V., Vidal J.V., Kubasov I.V., Kislyuk A.M., Kiselev D.A., Malinkovich M.D., Parkhomenko Y.N., Kobeleva S.P., Kholkin A.L., Sobolev N.A. Highly sensitive magnetic field sensor based on a metglas/bidomain lithium niobate composite shaped in form of a tuning fork. *Journal of Magnetism and Magnetic Materials*. 2019; 486. https://doi.org/10.1016/j.jmmm.2019.04.061
52. Vidal J.V., Turutin A.V., Kubasov I.V., Kislyuk A.M., Malinkovich M.D., Parkhomenko Y.N., Kobeleva S.P., Pakhomov O.V., Sobolev N.A., Kholkin A.L. Low-frequency vibration energy harvesting with bidomain $LiNbO_3$ single crystals. *IEEE Transactions on Ultrasonics, Ferroelectrics, and Frequency Control*. 2019; 66(9): 1480–1487. https://doi.org/10.1109/tuffc.2019.2908396
53. Vidal J.V., Turutin A.V., Kubasov I.V., Kislyuk A.M., Kiselev D.A., Malinkovich M.D., Parkhomenko Y.N., Kobeleva S.P., Sobolev N.A., Kholkin A.L. Dual vibration and magnetic energy harvesting with bidomain $LiNbO_3$-based composite. *IEEE Transactions on Ultrasonics, Ferroelectrics, and Frequency Control*. 2020; 67(6): 1219–1229. https://doi.org/10.1109/tuffc.2020.2967842
54. Godau C., Kämpfe T., Thiessen A., Eng L.M., Haußmann A. Enhancing the domain wall conductivity in lithium niobate single crystals. *ACS Nano*. 2017; 11(5): 4816–4824. https://doi.org/10.1021/acsnano.7b01199
55. Volk T.R., Gainutdinov R.V., Zhang H.H. Domain-wall conduction in AFM-written domain patterns in ion-sliced $LiNbO_3$ films. *Applied Physics Letters*. 2017; 110(13): 1–6. https://doi.org/10.1063/1.4978857

56. Schröder M., Chen X., Haußmann A., Thiessen A., Poppe J., Bonnell D.A., Eng L.M. Nanoscale and macroscopic electrical ac transport along conductive domain walls in lithium niobate single crystals. *Materials Research Express* 2014; 1(3): 035012. https://doi.org/10.1088/2053-1591/1/3/035012
57. Jorgensen P.J., Bartlett R.W. High temperature transport processes in lithium niobate. *Journal of Physics and Chemistry of Solids*. 1969; 30(12): 2639–2648. https://doi.org/10.1016/0022-3697(69)90037-7
58. Limb Y., Cheng K.W., Smyth D.M. Composition and electrical properties in $LiNbO_3$. *Ferroelectrics*. 1981; 38(1): 813–816. https://doi.org/10.1080/00150198108209546
59. Schirmer O.F., Thiemann O., Wöhlecke M. Defects in $LiNbO_3$–I. Experimental aspects. *Journal of Physics and Chemistry of Solids*. 1991; 52(1): 185–200. https://doi.org/10.1016/0022-3697(91)90064-7
60. Garcia-Cabanes A., Dieguez E., Cabrera J.M., Agullo-Lopez F. Contributing bands to the optical absorption of reduced $LiNbO_3$: thermal and optical excitation. *Journal of Physics: Condensed Matter*. 1989; 1(36): 6453–6462. https://doi.org/10.1088/0953-8984/1/36/013
61. Bordui P.F., Jundt D.H., Standifer E.M., Norwood R.G., Sawin R.L., Galipeau J.D. Chemically reduced lithium niobate single crystals: Processing, properties and improved surface acoustic wave device fabrication and performance. *Journal of Applied Physics.* 1999; 85(7): 3766–3769. https://doi.org/10.1063/1.369775
62. Arizmendi L., Cabrera J.M., Agullo-Lopez F. Defects induced in pure and doped $LiNbO_3$ by irradiation and thermal reduction. *Journal of Physics C: Solid State Physics*. 1984; 17(3): 515–529. https://doi.org/10.1088/0022-3719/17/3/021
63. Shi J., Fritze H., Weidenfelder A., Swanson C., Fielitz P., Borchardt G., Becker K.-D. Optical absorption of electronic defects and chemical diffusion in vapor transport equilibrated lithium niobate at high temperatures. *Solid State Ionics.* 2014; 262: 904–907. https://doi.org/10.1016/j.ssi.2013.11.025
64. Esin A.A., Akhmatkhanov A.R., Shur V.Y. The electronic conductivity in single crystals of lithium niobate and lithium tantalate family. *Ferroelectrics*. 2016; 496(1): 102–109. https://doi.org/10.1080/00150193.2016.1157438
65. Shportenko A.S., Kislyuk A.M., Turutin A.V., Kubasov I.V., Malinkovich M.D., Parkhomenko Y.N. Effect of contact phenomena on the electrical conductivity of reduced lithium niobate. *Modern Electronic Materials*. 2021; 7(4): 167–175. https://doi.org/10.3897/j.moem.7.4.78569
66. Kislyuk A.M., Ilina T.S., Kubasov I.V., Kiselev D.A., Temirov A.A., Turutin A.V., Malinkovich M.D., Polisan A.A., Parkhomenko Y.N. Tailoring of stable induced domains near a charged domain wall in lithium niobate by probe microscopy. *Modern Electronic Materials*. 2019; 5(2): 51–60. https://doi.org/10.3897/j.moem.5.2.51314
67. Lushkin A.Y., Nazarenko V.B., Pilipchak K.N., Shnyukov V.F., Naumovets A.G. The impact of annealing and evaporation of crystals on their surface composition. *Journal of Physics D: Applied Physics*. 1999; 32(1): 9–15. https://doi.org/10.1088/0022-3727/32/1/003
68. Schirmer O. F., Imlau M., Merschjann C., Schoke B. Electron small polarons and bipolarons in $LiNbO_3$. *Journal of Physics: Condensed Matter*. 2009; 21(12): 123201. https://doi.org/10.1088/0953-8984/21/12/123201
69. Dutt D.A., Feigl F.J., DeLeo G.G. Optical absorption and electron paramagnetic resonance studies of chemically reduced congruent lithium niobate. *Journal of Physics and Chemistry of Solids*. 1990; 51(5): 407–415. https://doi.org/10.1016/0022-3697(90)90175-F
70. Jhans H., Honig J.M., Rao C.N.R. Optical properties of reduced $LiNbO_3$. *Journal of Physics C: Solid State Physics*. 1986; 19(19): 3649–3658. https://doi.org/10.1088/0022-3719/19/19/019
71. Imlau M., Badorreck H., Merschjann C. Optical nonlinearities of small polarons in lithium niobate. *Applied Physics Reviews*. 2015; 2(4): 040606. https://doi.org/10.1063/1.4931396